

RF Pulse Signal Integrity Analysis for Nonlinear Ended Microstrip Line Atom-Probe Tomography

L. Zhao¹, A. Delamare¹, A. Normand¹, F. Delaroche¹, O. Latry¹, F. Vurpillot¹,
B. Ravelo²

¹ UMR CNRS 6634 - Normandy University GPM, Université and INSA de Rouen, Saint-Etienne-du-Rouvray, France

² IRSEEM EA 4353, at the Graduate School of Engineering, ESIGELEC, Saint-Etienne-du-Rouvray, France

E-mail: lu.zhao@univ-rouen.fr

Abstract. A signal integrity (SI) analysis of high voltage rectangular short pulses for the atom-probe system is explored in this paper. The operated RF transient pulse is considered for exciting on material sample inside an ultra-high vacuum (UHV) cryogenic chamber. The ns-duration pulse signal is injected into the cryogenic analysis chamber through the transmitting system mainly constituted by a microstrip interconnect line ended by optical controlled nonlinear load. The whole system frequency characterization is performed based on the S-parameter measurements. As expected, a challenging ultra-short rectangular shape pulse is exhibited by the pulser. Promising experimental results with the improvement of ion mass spectrum is demonstrated with the designed RF pulser.

1. INTRODUCTION

Atom probe tomography is a nanoscale analysis technique for material science. It is now widely spread in the nano-characterization world. One of the key performances of the modern instrument is its mass resolving power. Indeed, recent study on atom-probe [1] demonstrated that a ns-duration rectangular voltage pulse could improve the analysis capability of this scientific instrument. Different techniques can be deployed to generate such a short duration pulse. A pulse generator concept [2] using photoconductive switches has been generally used for producing ultra-short pulses with rise-time in ps-scale and sub-ns duration [3], [4]. In the field of pulsed power technique, the rise-/fall time is mainly depended on the switching speed of high power switch. The optical technique has more advantage than conventional electronic techniques. Photoconductive semiconductor switches thus are very suitable candidate for the high-power pulsed application because they are simple, faster switching speed and jitter-free response etc. Among the numbers of PCSS material, the silicon PCSS is chosen for the application because of its linear response and simple integration[5].

In this paper, an improved atom-probe system constituted by a rectangular shape pulse generator presenting ns full width is examined. The signal integrity (SI) investigation will be carried out by considering the S-parameters and the transient behaviours of the transmitted ns-duration FW pulse.



2. CONFIGURATION OF THE ns-PULSE GENERATOR ATOM-PROBE UNDER STUDY

A needle-like sample introduced in a vacuum chamber (10^{-10} mbar) and maintained low cryogenic temperatures (~ 80 K), the atoms on the sample surface are eroded by means of negative HV pulses applying on the local electrode which is placed very close to the sample (< 1 mm) [1][6]. A position-sensitive detector in front of the sample (10-20cm) permits identifying the atomic specie by the time-of-flight mass spectrometry [6]. Due to the stochastic nature of the field evaporation process (the physical phenomenon inducing the atom by atom erosion), it degrades the mass resolution of atom-probe. Therefore, the time-domain behaviour of the field evaporation which can be controlled with the excitation pulse voltage can be a key element for the atom-probe improvement. The innovative pulse generator solution with challenging rise-/fall-time investigated in this paper is mainly based on the nonlinear loaded microstrip transmission line (TL) using photoconductive switch (PCSS). An HV rectifier diode sustaining up to 4kV DC is employed and associated with an amplified Ti: Sa fs laser (provided by Quantronic IntegraE®) served as an optical command. The ns-pulse generator under study is overviewed in Figure 1. The PCSS ended microstrip TL printed on the FR4 substrate having relative permittivity $\epsilon_r=4.4$ and thickness $h=1.6$ mm can be seen in left of Figure 1. The $V_0=6$ kV DC driven source resistance was fixed to $R_s=10$ k Ω . In difference with the generator proposed in [7], a nonlinear load constituted by the PCSS is inserted in upstream of the termination $R_0=50\Omega$. The PCSS is controlled by an optical beam in order to deliver the stored energy into the load resistance. Then, a ps range rise time electric pulse can be generated across R_0 [7].

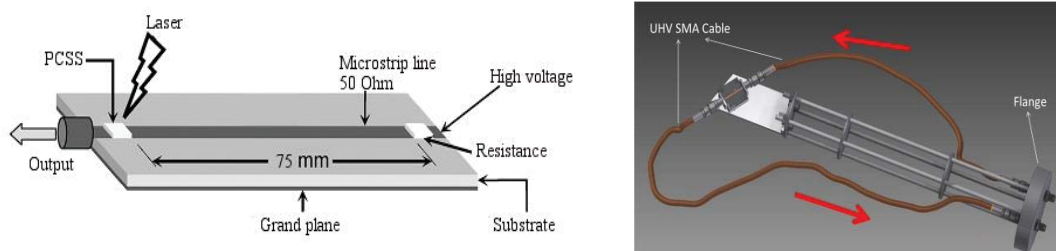


Figure 1. Nonlinear loaded microstrip generator (in left) and the transmitting system (in right).

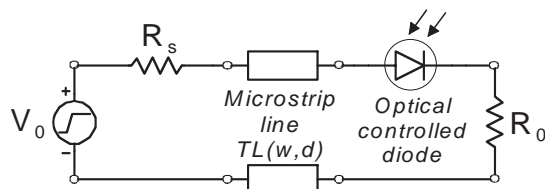


Figure 2. Equivalent schematic of atom-probe pulser.

The ns rectangular pulses can be obtained with laser energy $20\mu\text{J}/\text{pulse}$. The pulse generator output is connected to the input of the transmitting system as depicted in the right of Figure 1. For the basic SI analysis, the pulse generator microstrip structure was assumed as equivalent to the electrical circuit schematized in Figure 2.

As illustrated in right of Figure 1, the proposed atom-probe generator transmitting pulse system is essentially composed of the microstrip circuit interconnected to the UHV SMA cables. The microstrip TL is laminated with Copper conductor presenting $35\mu\text{m}$ thickness having physical width $w=3$ mm and length $d=75$ mm. The centre of the microstrip TL is pierced with via presenting diameter $\varnothing=300\mu\text{m}$. This hole serves as a microelectrode, and the sample directly be excited by the electrical pulse, atoms are fielded evaporated from the sample and are projected through the hole to the position sensitive detector placed about 20cm in front of the device.

3. INVESTIGATION ON THE OPERATED ns-DURATION PULSE SIGNAL INTEGRITY WITH S-PARAMETERS ANALYSIS

With the previously described generator, we expected to exhibit 1ns full width half maximum (FWHM) rectangular shape voltage to excite the material sample. To do this, the PCSS was excited with fs

duration laser pulse. The different blocks of the generator S-parameter responses and the time-domain plot of the pulse will be explored in the next paragraphs.

3.1. ns-Duration Rectangular Shape Pulse Generation

First and foremost, after injecting the slightly distorted rectangular shape pulse plotted in left of Figure 3-1 into the UHV chamber by the transmitting system, the output signal plotted in dashed line was observed. It is noteworthy that the measurement was performed with the Agilent® infiniium 54855A oscilloscope. As the transmitting system behaves as low-pass filter behavior, the high order harmonics was attenuated. The corresponding spectra obtained from Fast Fourier Transform (FFT) of measured signal from oscilloscope are displayed in the right of Figure 3-1. It illustrates that the system loss occurs from 1.5GHz, and due to the oscilloscope bandwidth limit, the spectra is vanished from 6GHz.

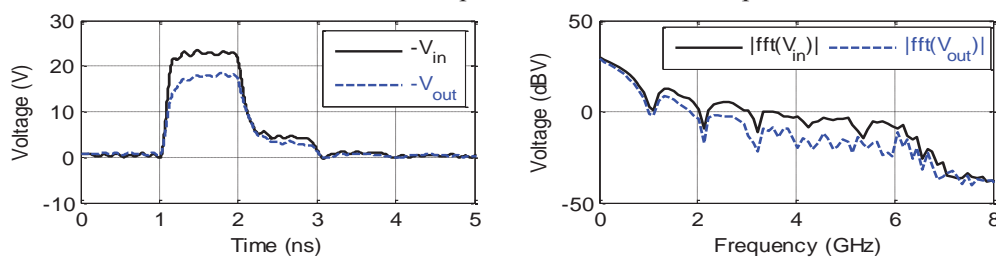


Figure 3-1. Transient signals before and after passing the transmitting system: dash line is the input and dash dot line is the output and the corresponding FFT.

3.2. Transmitting System Characterization

To investigate the frequency limitation and matching problem of assembled two-port transmitting system, the return and insertion losses S_{11} and S_{21} were measured up to 8GHz by using the ENA E5071B VNA for the UHV SMA cables, the flange and the 2-port transmitting system, respectively. The frequency dependent results are displayed in the Figure 3-2. Note that the insertion loss of the whole system is due to limitation of the flange and the vacuum cables at high frequency range. Moreover, S_{21} is below -3dB above 1.5GHz. It means that most of energy (more than 50%) was not transmitted over the upper frequency band.

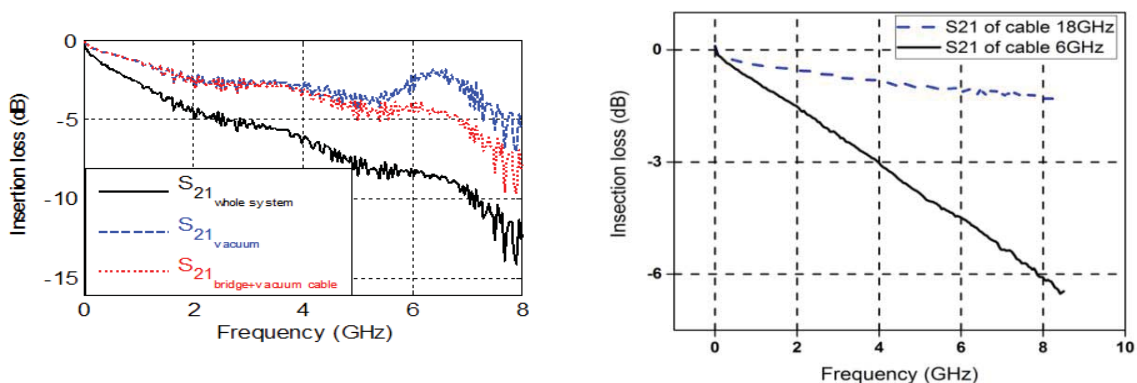


Figure 3-2. S_{21} of the access line system including the UHV SMA, cable and the flange (in left) and the insertion loss (S_{21}) of different UHV SMA cables (in right).

The insertion loss (S_{21}) of UHV SMA cables is compared in the right of Figure 3-2. Although the indicated bandwidth of cable is 6GHz by manufacturer, the effective bandwidth is only 4GHz in practice.

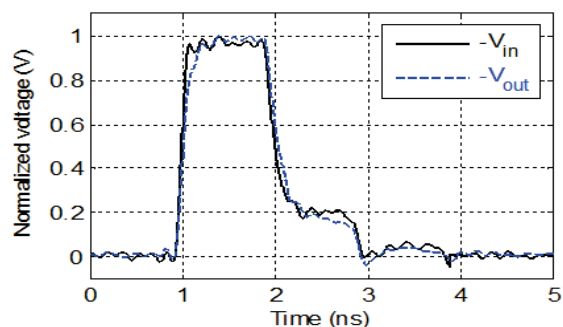


Figure 3-3. Signals measured after replacing the UHV SMA cable.

3.3. Mass Spectrum Improvement Application

Although rectangular pulses with ns duration are not very well transmitted by the system, the voltage pulse applied to the sample could be a Gaussian-similar pulse. Preliminary mass spectrum obtained by analysing Al sample ($M=27\text{uma}$) with standard voltage pulse and with sub-ns short pulses demonstrates a significant improvement of the mass resolution power. Comparing to the standard atom-probe, the pulse transmitting system installed in atom probe displayed in Figure 4. The experimental result shows that the mass resolution is 3 times better than that obtained by the standard atom probe.

Considering all the system, we proposed to replace the UHV SMA cables with another one having much larger bandwidth of 18GHz as a simple way to improve the transmission shown in the right of Figure 3-2. As expected, a significant improvement was realized which can be seen with the transient plot shown in Figure 3-3. Practical transmission efficiency with rectangular shape pulse presenting rise time better than 200ps is realized.

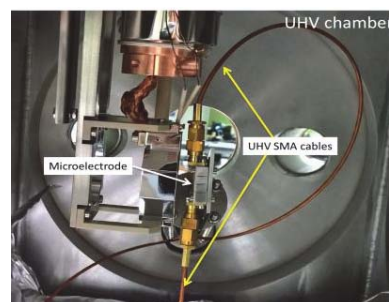


Figure 4. Photography of atom probe analysis chamber with proposed microstrip TL (microelectrode).

4. CONCLUSION

A new method to improve the atom-probe tomography based on RF transient ns-pulse generator using nonlinear ended microstrip TL with PCSS is developed. The transmitting system has been investigated in frequency domain. The signal distortion is largely due to the combined effect of the UHV SMA cable and the flange. To avoid the transmission problem, a sub-ns rectangular shape pulse generator adapted to the UHV chamber is needed so that the generated voltage pulses can be applied directly to the sample.

5. REFERENCE

- [1] Zhao L, Normand A, Delaroche F, Ravelo B and Vurpillot F 2015 *Int J Mass Spectrom* **386** pp 47–53
- [2] Vergne B, Couderc V, Barthélémy A, Lalande M, Bertrand V and Gontier D 2007 *Dig Tech Pap Int Pulsed Power Conf* pp 818–823
- [3] Auston D H 1975 *Appl Phys Lett* **101** pp 24–27
- [4] El Amari S, Kanaan M, Merla C, Vergne B, Arnaud-Cormos D, Leveque P and Couderc V 2010 *IEEE Photonics Technol Lett* **22** (21) pp 1577–1579
- [5] Amari S E L 2010 Développement et caractérisation de générateur optoélectronique d'impulsions de champ électrique nanoseconde et subnanoseconde de forte intensité : application au domaine biomédical (in French), *PhD thesis*, Univ. Limoges, France
- [6] Miller M K 2014 *Atom Probe Tomography: the Local Electrode Atom Probe* **10** (S02)
- [7] Lee C H 1990 *IEEE Trans Microw Theory Tech* **38** (5) pp 596–607